Effective quantum equations for the semiclassical description of the Hydrogen atom

Guillermo Chacón-Acosta

Departamento de Matemáticas Aplicadas y Sistemas, Universidad Autónoma Metropolitana-Cuajimalpa, México D. F. 01120, México

E-mail: gchacon@correo.cua.uam.mx

Héctor H. Hernández

Universidad Autónoma de Chihuahua, Facultad de Ingeniería, Nuevo Campus Universitario, Chihuahua 31125, México

E-mail: hhernandez@uach.mx

Abstract. We study the Hydrogen atom as a quantum mechanical system with a Coulomb like potential, with a semiclassical approach based on an effective description of quantum mechanics. This treatment allows us to describe the quantum state of the system as a system of infinite many classical equations for expectation values of configuration variables, their moments and quantum dispersions. It also provides a semiclassical description of the orbits and the evolution of observables and spreadings and their back-reaction on the evolution.

PACS numbers: 03.65.-w, 03.65.Sq

1. Introduction

It is known from general principles [1] that the evolution of the expectation value of the position operator in a general quantum state is given by Ehrenfest's theorem, which is the quantum analogue of Newton's second law. It can be written as $m\frac{d^2\langle\hat{x}\rangle}{dt^2} = \left\langle \hat{F}\left(\hat{x}\right)\right\rangle$. We notice immediately that although the left hand side corresponds to the classical expression, the right hand side does not, instead we have a non-local force term which, in principle, can be interpreted statistically. When we expand this term in Taylor series we notice that it contains infinite quantum corrections that are expressed as powers of the dispersions:

$$\left\langle \hat{F}\left(\hat{x}\right)\right\rangle = F\left(\langle\hat{x}\rangle\right) + \frac{1}{2}\Delta x^2 F''\left(\langle\hat{x}\rangle\right) + \dots$$

The momentous quantum mechanics is based on the same idea applied to any operator [2]. It is similar to the low energy effective action method which has been largely and successfully used in quantum field theory. There, the actions of interacting theories can be seen as quantum corrections to the classical action [3]. Indeed, in some circumstances, the effective equations reproduce the results of the effective action even better than the well known WKB approximation [4].

The effective equations approach for quantum systems has been developed to systematically analyze quantum effects through quantum induced corrections to classical equations, leading to observable phenomena as deviations from the semi-classical behavior [2]. These quantum corrections come from quantum backreaction effects. It has been successfully applied to an isotropic and homogeneous model in loop quantum cosmology [5], which has been used to predict the evolution of the universe before the Big Bang [6]. It has also been successfully used to analyze cosmological isotropic models with matter [7] and with positive cosmological constant [8], and also to study the effective constriction equations for loop gravity and relativistic systems [9].

Effective equations describe the behavior of the expectation values in a definite state, replacing the description in terms of the Schrödinger equation by a system of infinite coupled equations for both classical variables and quantum fluctuations. These equations are particularly suitable for semi-classical states, which may shed some light on effects that could be potentially observable. Moreover, in those states, the system of infinite equations can be reduced to a finite one by making some consistent truncations, as for example in adiabatic approximation.

For some systems like the harmonic oscillator [2] it is possible to determine the exact properties in some state because the second-order moments form a closed system and because they decouple from the classical variables. For more complicated systems (e.g. anharmonic systems) the equations for both classical and quantum variables are highly coupled, so it will require additional approximations for the equations.

In this work we use the momentous method to obtain the effective description of a standard spinless quantum system with a Coulomb potential, i.e. a hydrogen atom. In section 2 we describe this version of quantum mechanics with the introduction of

the moments or fluctuations as additional variables that encode the quantum degrees of freedom. We describe the construction of the quantum Hamiltonian, first for one dimensional systems and also for higher dimensions. We also compute the equations of motion for the expectation values of basic operators for which the main ingredient is the calculation of the Poisson algebra between quantum variables. In section 3 we compute the quantum Hamiltonian for this system that corresponds to the classical Kepler problem with correction terms. With this Hamiltonian we write the corresponding effective equations up to second order in the moments, finding twelve coupled equations: three for the classical variables and nine for all the relevant moments. In section 4, we solve numerically the system of effective equations and analyze the quantum corrected behavior of the system comparing it qualitatively to the classical case. Finally in section 5 we summarize and discuss our results.

2. Effective dynamics of quantum systems: Momentous quantum mechanics

Effective equations of quantum systems describe the dynamics of expectation values of observables, as well as the evolution of its dispersions. These equations allow us to study the quantum evolution by analyzing how quantum effects modify classical dynamics. In regimes where the fluctuations and dispersions are small with respect to observables one can treat the quantum effects perturbatively thus providing the ideal scenario to perform numerical analysis in a semiclassical regime [2].

Equations of motion in effective theory are derived from an effective Hamiltonian, treating expectation values of observables and their associated momenta as classical canonical variables. Quantum fluctuations are introduced as a set of new *quantum* dynamical variables defined as follows:

$$G^{a,b} \equiv \left\langle (\hat{x}-x)^a (\hat{p}-p)^b \right\rangle_{\text{Weyl}}, \quad a+b \geq 2 \tag{1}$$

where $x \equiv \langle \hat{x} \rangle$ and $p \equiv \langle \hat{p} \rangle$, and the subscript indicates that the operators inside the brackets are Weyl (or completely symmetrical) ordered. This quantum variables describe the spreading of the quantum modified evolution from the classical one.

The momenta are not arbitrary but subject to generalized uncertainty relations such as

$$G^{2,0}G^{0,2} - (G^{1,1})^2 \geq \frac{\hbar^2}{4}. \tag{2}$$

Notice that $G^{2,0}$ and $G^{0,2}$ are the standard dispersions Δx^2 and Δp^2, and that (2) simplifies to the usual uncertainty principle for pure states [1].

Evolution is obtained by evaluating Poisson brackets of variables and momenta with the *quantum* effective Hamiltonian that is defined as the expectation value of the standard Hamiltonian operator

$$\langle \hat{H} \rangle \equiv H_Q = H(x,p) + \sum_{a,b} \frac{1}{a!b!} \frac{\partial^{a+b} H}{\partial x^a \partial p^b} G^{a,b}, \tag{3}$$

where $H(x,p)$ is the classical Hamiltonian. Equations of motion are obtained in the usual Hamiltonian formulation $\dot{f} = \{f, H_Q\}$. Quantum variables $G^{a,b}$ are now dynamical, as the classical ones (x,p). For general models one obtains an infinitely coupled system of equations with infinitely many variables that, however complicated, provides us a full description of the system. It is also important to note that the effective equations so obtained are state dependent, since the dynamic quantum fluctuations affect the behavior of the expectation values.

To obtain effective equations of motion one compute the Poisson brackets of variables with the quantum-corrected Hamiltonian: the following relations, for one degree of freedom, are useful

$$\{x,p\} \quad = 1, \tag{4}$$

$$\{x, G^{a,b}\} = 0, \tag{5}$$

$$\{p, G^{a,b}\} = 0. \tag{6}$$

The Poisson algebra for the moments was originally obtained in [2] but was recently reexamined in [8] for its algebraic and numerical implementation

$$\{G^{a,b}, G^{c,d}\} = adG^{a-1,b}G^{c,d-1} - bcG^{a,b-1}G^{c-1,d} + \\ + \sum_n \left(\frac{i\hbar}{2}\right)^{n-1} K^n_{abcd} G^{a+c-n,b+d-n}, \tag{7}$$

where the sum runs over odd numbers from $n = 1 \ldots \tilde{N}$, with $1 \leq \tilde{N} < \min[a+c, b+d, a+b, c+d]$, and the coefficient is

$$K^n_{abcd} = \sum_{s=0}^{n} (-1)^s s!(n-s)! \begin{pmatrix} a \\ s \end{pmatrix} \begin{pmatrix} b \\ n-s \end{pmatrix} \begin{pmatrix} c \\ n-s \end{pmatrix} \begin{pmatrix} d \\ s \end{pmatrix}. \tag{8}$$

For the quantum harmonic oscillator it was shown that the ground state energy is added to the classical Hamiltonian [2], [10]. It was also seen that the system is solvable since the moments are not coupled with the expectation values of classical variables: there is no quantum back-reaction. In the case of anharmonic systems, one can use an adiabatic approximation that produces effective forces coming from the coupling terms between the expectation variables and the moments. This method has also been applied to the isotropic and homogeneous model in loop quantum cosmology [5, 6], and to study different cosmological models with matter [7], cosmological constant [8], among others.

For the case of k pairs of canonical degrees of freedom we have the general definition for quantum variables:

$$G^{a_1,b_1,\ldots,a_k,\ldots,b_k} \equiv \left\langle (\hat{x}_1 - x_1)^{a_1} (\hat{p}_1 - p_1)^{b_1} \cdots (\hat{x}_k - x_k)^{a_k} (\hat{p}_k - p_k)^{b_k} \right\rangle_{\text{Weyl}} \tag{9}$$

where $a_i + b_i \geq 2$ and $i = 1, \ldots, k$. We have $G^{0,0,\ldots,0,0} = 1$, $G^{0,\ldots,a_j,\ldots,0} = 0$. We may also note that we will always have an even number of indices and each pair (a_i, b_i) corresponds to the moments of each canonical pairs (x_i, p_i).

The generalized quantum-corrected effective Hamiltonian is as follows

$$H_Q := \sum_{a_1,b_1}^{\infty} \cdots \sum_{a_k b_k}^{\infty} \frac{1}{a_1!b_1! \cdots a_k!b_k!} \frac{\partial^{a_1+b_1+\ldots+a_k+b_k} H}{\partial x_1^{a_1} \partial p_1^{b_1} \ldots \partial x_k^{a_k} \partial p_k^{b_k}} G^{a_1,b_1;\ldots;a_k,b_k} \tag{10}$$

With this Hamiltonian we will obtain the evolution equations for each degree of freedom. For this we need the set of Poisson brackets: those among the expectation values are known and those between the expectation values and moments vanish.

The Poisson algebra among the moments is the generalization of equation (7); this expression was first found in [2] and then corrected in [8]

$$\begin{aligned}\{G^{a_1,b_1;\ldots;a_k,b_k}, G^{c_1,d_1;\ldots;c_k,d_k}\} = &\sum_{i=1}^{k}\Big(a_i d_i G^{a_1,b_1;\ldots;a_i-1,b_i;\ldots;a_k,b_k} G^{c_1,d_1;\ldots,c_i,d_i-1;\ldots;c_k,d_k} - \\ &b_i c_i G^{a_1,b_1;\ldots;a_i,b_i-1;\ldots;a_k,b_k} G^{c_1,d_1;\ldots;c_i-1,d_i;\ldots;c_k,d_k}\Big) \\ &+\sum_{n}\sum_{s}\sum_{e_1,\ldots,e_k}(-1)^s\left(\frac{i\hbar}{2}\right)^{n-1}\delta_{\sum_i e_i,n} \\ &\times \mathcal{K}^{n,s,\{e\}}_{\{a\},\{b\},\{c\},\{d\}} G^{a_1+c_1-e_1,b_1+d_1-e_1;\ldots;a_k+c_k-e_k,b_k+d_k-e_k}\end{aligned} \tag{11}$$

$n = 1, \ldots, \tilde{N}$, and

$$\tilde{N} = \begin{cases} 1, & \sum_i(\min[a_i,d_i]+\min[b_i,c_i]) \leq 1, \\ \sum_i(\min[a_i,d_i]+\min[b_i,c_i]) - 1, & \sum_i(\min[a_i,d_i]+\min[b_i,c_i]) > 1. \end{cases} \tag{12}$$

$s = 0, \ldots, n\,;\ 0 \leq e_i \leq \min[a_i, d_i, s] + \min[b_i, c_i, n-s]$.

The $\mathcal{K}$ coefficient is

$$\mathcal{K}^{n,s,\{e\}}_{\{a\},\{b\},\{c\},\{d\}} = \sum_{g_1,\ldots,g_k}\frac{\delta_{\sum_i g_i,n-s}}{s!(n-s)!}\prod_i \frac{\binom{a_i}{e_i-g_i}\binom{b_i}{g_i}\binom{c_i}{g_i}\binom{d_i}{e_i-g_i}}{\binom{n-s}{g_i}\binom{s}{e_i-g_i}}, \tag{13}$$

where $\max[e_i - s, e_i - a_i, e_i - d_i, 0] \leq g_i \leq \min[b_i, c_i, n-s, e_i]$.

Henceforth we will consider the case $k = 2$, corresponding to a two dimensional problem, being the case for the Kepler system.

3. Effective quantum Hamiltonian for Coulomb potential

In non-relativistic quantum mechanics the hydrogen atom is studied with the Schrödinger equation with a central potential; when one considers stationary solutions it is possible to separate the angular and the radial parts and thus obtaining the corresponding eigenfunctions. It is well known that for the Coulomb potential $V(r) = -\frac{k}{r}$, with $k = \frac{e^2}{4\pi\epsilon_0}$, the radial function is the product of the associated Laguerre polynomials by a decaying exponential of r and r^l [1]. Moreover, the corresponding energy levels of the Hydrogen atom are $E_n = -\frac{k}{2a_0 n^2}$ in terms of the Bohr radius $a_0 = \frac{\hbar^2}{mk}$.

The Schrödinger treatment of the Hydrogen atom has long been known and solved [11]. The state of any quantum mechanical system in this picture is encoded in the

wave function $\psi(\mathbf{r},t)$, observables and expectation values are all obtained from the wave function considering it as the probability distribution for the system at hand.

We study now this system using the effective momentous method of quantum mechanics exposed in the previous section. We will analyze how the moments evolve in time and how they modify the corresponding classical dynamics.

The classical Hamiltonian for the Hydrogen atom is that of the Kepler problem

$$H(r,p) = \frac{p_r^2}{2m} + \frac{p_\theta^2}{2mr^2} - \frac{k}{r}, \tag{14}$$

which, by virtue of the conservation of angular momentum, is a two dimensional system with classical polar configuration variables (r,θ) and (p_r, p_θ) are their canonical conjugate momenta.

Using the definition (9) of the moments for our two pairs of canonical variables we have

$$G^{a,b,c,d} = \left\langle (\hat{r}-r)^a (\hat{p}_r - p_r)^b (\hat{\theta}-\theta)^c (\hat{p}_\theta - p_\theta)^d \right\rangle_{\text{Weyl}}, \tag{15}$$

from (10) we obtain the corresponding quantum effective Hamiltonian

$$H_Q = \frac{p_r^2}{2m} + \frac{p_\theta^2}{2mr^2} - \frac{k}{r} + \frac{G^{0,2,0,0}}{2m} + \frac{G^{0,0,0,2}}{2mr^2} + \sum_{a\geq 2}\left[\frac{p_\theta^2(a+1)}{2mr} - k\right]\frac{(-1)^a}{r^{a+1}}G^{a,0,0,0} + \sum_{b\geq 1}\frac{(-1)^b}{mr^{b+2}}(b+1)\left[p_\theta G^{b,0,0,1} + \frac{1}{2}G^{b,0,0,2}\right]. \tag{16}$$

The first three terms correspond to the classical Hamiltonian (14), the fourth term is the radial momentum dispersion, the fifth term is the angular momentum dispersion. The sum for $a \geq 2$ is associated with the fluctuations in the radial component, while the sum for $b \geq 1$ contains the coupled moments for the fluctuations in r and p.

As can be seen from (16) the system is highly coupled, in contrast with the case of the harmonic oscillator where the moments decouple from the expectation values and its contribution to the quantum Hamiltonian is constant, rendering the ground state energy $\frac{\hbar\omega}{2}$ [2]. The fact that for the central potential the moments can not be decoupled may hinder the calculation, however we will perform consistent truncations at different orders in quantum variables. We note that, to second order in the moments, the last term of the second sum does not appear, that is, in order to consider all the terms of the effective Hamiltonian to this order we need to consider at least the third order momenta.

We obtain the equations of motion for this set of variables by computing their Poisson brackets with the Hamiltonian (16). For expectation values

$$\dot{r} = \{r, H_Q\} = \frac{p_r}{m}, \tag{17}$$

$$\dot{p_r} = \{p_r, H_Q\} = \frac{p_\theta^2}{mr^3} - \frac{k}{r^2} + \frac{G^{0,0,0,2}}{mr^3} + \sum_{a\geq 2}(-1)^a\frac{(a+1)}{r^{a+2}}G^{a,0,0,0}\left[\frac{p_\theta^2}{2m}\frac{(a+2)}{r} - k\right] + \sum_{b\geq 1}(-1)^b\frac{(b+1)(b+2)}{mr^{b+3}}\left[p_\theta G^{b,0,0,1} + \frac{1}{2}G^{b,0,0,2}\right], \tag{18}$$

$$\dot{\theta} = \{\theta, H_Q\} = \frac{p_\theta}{mr^2} - \frac{2}{mr^3}G^{1,0,0,1} + \sum_{a\geq 2}\frac{(-1)^a(a+1)}{mr^{a+2}}\left[p_\theta G^{a,0,0,0} + G^{a,0,0,1}\right], \quad (19)$$

$$\dot{p_\theta} = \{p_\theta, H_Q\} = 0. \quad (20)$$

Equation (17) is just the usual definition of the momentum associated with r while equation (20) states the classical conservation of angular momentum, i.e. $p_\theta = l = const.$ One can see the strong quantum back-reaction of this semiclassical approach for classical variables in equations (18) and (19).

The equations of motion for moments at any order follow from (11):

$$\begin{aligned}\dot{G}^{a_1,b_1,a_2,b_2} = \{G^{a_1,b_1,a_2,b_2}, H_Q\} &= \frac{1}{2m}\{G^{a_1,b_1,a_2,b_2}, G^{0,2,0,0}\} + \frac{1}{2mr^2}\{G^{a_1,b_1,a_2,b_2}, G^{0,0,0,2}\} \\ &+ \sum_{a\geq 2}\left[\frac{p_\theta^2(a+1)}{2mr} - k\right]\frac{(-1)^a}{r^{a+1}}\{G^{a_1,b_1,a_2,b_2}, G^{a,0,0,0}\} \\ &+ \sum_{b\geq 1}\frac{(-1)^b}{mr^{b+2}}(b+1)\left[p_\theta\{G^{a_1,b_1,a_2,b_2}, G^{b,0,0,1}\} + \frac{1}{2}\{G^{a_1,b_1,a_2,b_2}, G^{b,0,0,2}\}\right]\end{aligned} \quad (21)$$

As a simplification we consider an expansion in equations (16)-(21) up to second order in quantum variables. The corresponding system is

$$\dot{r} = \frac{p_r}{m}, \quad (22)$$

$$\dot{p_r} = \frac{l^2}{mr^3} - \frac{k}{r^2} + \frac{G^{0,0,0,2}}{mr^3} + \frac{3}{r^4}G^{2,0,0,0}\left[\frac{l^2}{m}\frac{2}{r} - k\right] - \frac{6l}{mr^4}G^{1,0,0,1}, \quad (23)$$

$$\dot{\theta} = \frac{l}{mr^2} - \frac{2}{mr^3}G^{1,0,0,1} + \frac{3l}{mr^4}G^{2,0,0,0}, \quad (24)$$

$$\dot{G}^{1,1,0,0} = -\frac{1}{m}G^{0,2,0,0} + \left[\frac{3l^2}{2mr} - k\right]\frac{2}{r^3}G^{2,0,0,0} - \frac{2l}{mr^3}G^{1,0,0,1}, \quad (25)$$

$$\dot{G}^{2,0,0,0} = -\frac{2}{m}G^{1,1,0,0}, \quad (26)$$

$$\dot{G}^{0,2,0,0} = 4\left[\frac{3l^2}{2mr} - k\right]\frac{1}{r^3}G^{1,1,0,0} - \frac{4l}{mr^3}G^{0,1,0,1}, \quad (27)$$

$$\dot{G}^{0,0,1,1} = -\frac{1}{mr^2}G^{0,0,0,2} + \frac{2l}{mr^3}G^{1,0,0,1}, \quad (28)$$

$$\dot{G}^{0,0,2,0} = -\frac{2}{mr^2}G^{0,0,1,1} + \frac{4l}{mr^3}G^{1,0,1,0}, \quad (29)$$

$$\dot{G}^{0,0,0,2} = 0, \quad (30)$$

$$\dot{G}^{1,0,1,0} = -\frac{1}{m}G^{0,1,1,0} - \frac{1}{mr^2}G^{1,0,0,1} + \frac{2l}{mr^3}G^{2,0,0,0}, \quad (31)$$

$$\dot{G}^{1,0,0,1} = -\frac{1}{m}G^{0,1,0,1}, \quad (32)$$

$$\dot{G}^{0,1,0,1} = \left[\frac{3l^2}{2mr} - k\right]\frac{2}{r^3}G^{1,0,0,1} - \frac{2l}{mr^3}G^{0,0,0,2}, \quad (33)$$

$$\dot{G}^{0,1,1,0} = -\frac{1}{mr^2}G^{0,1,0,1} + \left[\frac{3l^2}{2mr} - k\right]\frac{2}{r^3}G^{1,0,1,0} + \frac{2l}{mr^3}\left(G^{1,1,0,0} - G^{0,0,1,1}\right),$$

(34)

where we already inserted $p_\theta = l = const.$.

One can see that if all the moments $G^{a,b,c,d}$ are set to zero, we recover the classical equations of motion. Equation (30) can immediately be solved $G^{0,0,0,2} = \Delta l^2 \equiv \text{const}$. Indeed, from (21) it can be seen that if $a_1 = b_1 = a_2 = 0$, $b_2 = n$, then $\dot{G}^{0,0,0,b_2}$ is always zero and all the dispersions of the angular momentum are constants, $\Delta l^n = const$. With this simplification the system reduces to a set of twelve coupled differential equations for classical and quantum variables. It is evident that we will not find non-spreading solutions as in the harmonic oscillator case [2, 10].

4. Evolution and quantum back-reaction

In this section we analyze the evolution and quantum-corrected behavior of the system under consideration according to equations (22)-(34). We discuss two cases of interest.

4.1. Zero angular momentum

The case $l = 0$ corresponds to the so called one dimensional Hydrogen atom. Although one might think that this system as physically uninteresting it actually has interesting features [12]. It has been used to model Hydrogen atoms in the presence of strong magnetic fields as in astrophysical systems; it is also useful in modeling Rydberg atoms in external fields, the behavior of certain electrons near the surface of helium [13].

Classically this case reduces to a one-dimensional problem with radial equations:

$$\dot{r} = \frac{p_r}{m}, \qquad \dot{p_r} = -\frac{k}{r^2}. \tag{35}$$

As it evolves in time the position of the particle begins to increase as its velocity decreases, after that the radius starts to decrease as the velocity increases in the opposite direction (see Fig. 1). In Fig. 2, we show the phase space of the system in which these features are clear.

However, it turns out that the quantum corrected behavior, up to second order in the moments, is not reduced to a one effective dimension when $l = 0$. As we can see from equations (22)-(34), by setting $l = 0$, and even $\Delta l^n = 0$, there are still quantum fluctuations related to the angular momentum as G^{r,p_θ} and G^{p_r,p_θ}, from equations (32) and (33), which are not necessarily zero. This is not surprising since, from (9), we see that the term G^{r,p_θ} is

$$G^{r,p_\theta} = G^{1,0,0,1} = \langle (\hat{r} - r)(\hat{p}_\theta - p_\theta) \rangle_{\text{Weyl}} = \langle \hat{r}\ \hat{p}_\theta \rangle - lr, \tag{36}$$

and similarly for G^{p_r,p_θ}; these terms do not vanish. Indeed, from equation (24) we notice that $\dot{\theta}$ does not vanish but is proportional to G^{r,p_θ}. This implies that quantum fluctuations induce a two-dimensional motion in the system, modifying the classical behavior of r and p_r, as shown in Fig. 1 and 2. The two dimensional quantum-corrected behavior of $\theta(t)$ is shown in Fig. 3a. In Fig. 3b it is clear that the actual orbit is

(a) (b)

Figure 1. (a) The position $r(t)$ and (b) the momentum $p_r(t)$ as functions of time, for $l = 0$. The dashed (red) line corresponds to the classical behavior for $m = k = 1$. The other curves correspond to the second order effective quantum behavior; when $\Delta l^2 = 0$, solid (blue) curve and for $\Delta l^2 \neq 0$ dot-dashed (blue) curve.

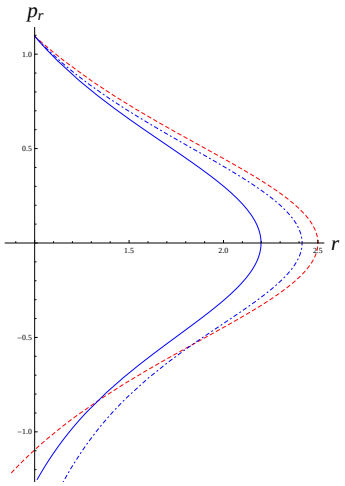

Figure 2. Classical and quantum corrected phase space for $l = 0$. The dashed (red) is the classical behavior, the quantum evolution for $\Delta l^2 = 0$, solid (blue) curve and for $\Delta l^2 \neq 0$ dot-dashed (blue) curve.

not one-dimensional but two-dimensional. This is a purely quantum effect that has no classical parallel.

If we consider $l \neq 0$ in the quantum-corrected equations of motion, we notice that the system is effectively two dimensional in the classical sense. If we look at equation (24) we see that in addition to the term G^{r,p_θ}, there are also two other contributions proportional to $G^{r,r}r^{-4}$ and r^{-2} not present when $l = 0$. The expectation value of products of linear and angular momentum operators in general do not commute, therefore the angular equation does not vanish. We see here that, at the semiclassical effective level, the classical observables acquire quantum corrections that are not negligible and that back-react latter on the classical variables.

This system does not correspond exactly to the effective description of the one dimensional Hydrogen atom. To be so all moments related to angular variables would

(a) (b)

Figure 3. (a) Effective quantum evolution of $\theta(t)$ and (b) the quantum modified orbit, for $l = 0$ and $m = k = 1$, $\Delta l^2 = 0$ solid (blue) curve and $\Delta l^2 \neq 0$ dot-dashed (blue).

necessarily equate to zero. Amusingly, when we impose this in our analysis we notice that the corresponding solution has qualitatively the same behavior as in Fig. 1, although in this case the motion is purely one dimensional.

4.2. Full two dimensional case

In standard quantum mechanics energy levels are obtained by solving the radial Schrödinger equation and imposing asymptotic conditions on the solution [11]. Observables Q are then obtained from the wave function $\psi(\mathbf{r})$ (for stationary solutions) in the usual way as its expectation values $Q = \langle \hat{Q} \rangle = \int \psi^* \, \hat{Q}\psi \, d^3x$.

The approach based in effective equations treats the dispersions as quantum corrections to the evolution. Because dispersions also evolve in time, we must analyze whether our considerations are valid, i.e., whether the quantum variables can be considered as perturbations, and under what circumstances. Our main goal is to study the evolution of expectation values and its deviation from the classical picture, then we now proceed to solve numerically equations (22)-(34).

In Fig. 4a it can be seen that for initial conditions that consider small enough dispersions, there is a region close to $t = 0$ where the dispersions are small compared to the classical variables, allowing a perturbative evolution. Furthermore, we notice in Fig. 4b, that for large times the radial coordinate oscillates with small amplitude around $r = 1$. The angular variable and its dispersion have a similar behavior.

Note that, as the fluctuations evolve, they begin to grow until they are comparable or even bigger to the expectation values. In this region they could no longer be considered as perturbations.

For $p_r/\sqrt{G^{p_r p_r}}$ we can see a similar oscillatory evolution in Fig. 5, for the same initial conditions. In the first part a perturbative approximation can be implemented while for larger times, it oscillates around zero with small amplitude. The effective radial momentum as compared with the classical one, starts close to it but as time increases the momentum becomes larger as well as its oscillation frequency. Again this implies that for large times the dispersion are of the same magnitude as the momentum.

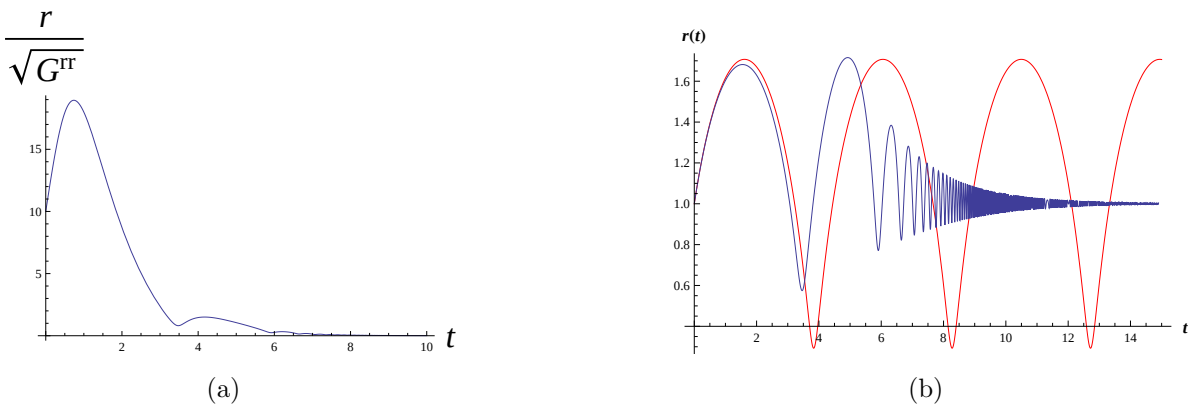

(a) (b)

Figure 4. (a) Plot of $r/\sqrt{G^{rr}}$ with initial conditions that consider small enough values for dispersions. (b) The radial coordinate as a function of time. Compared with the classical behavior, the effective one has a decreasing amplitude as evolves, and for large times oscillates around $r = 1$. In this plots we consider $m = 1$, $k = 2$ and $l = 1$. The initial conditions for unperturbed curves are $r = 1$, $p_r = 1$ and $\theta = \pi$; and for the moments we consider all of order 0.01.

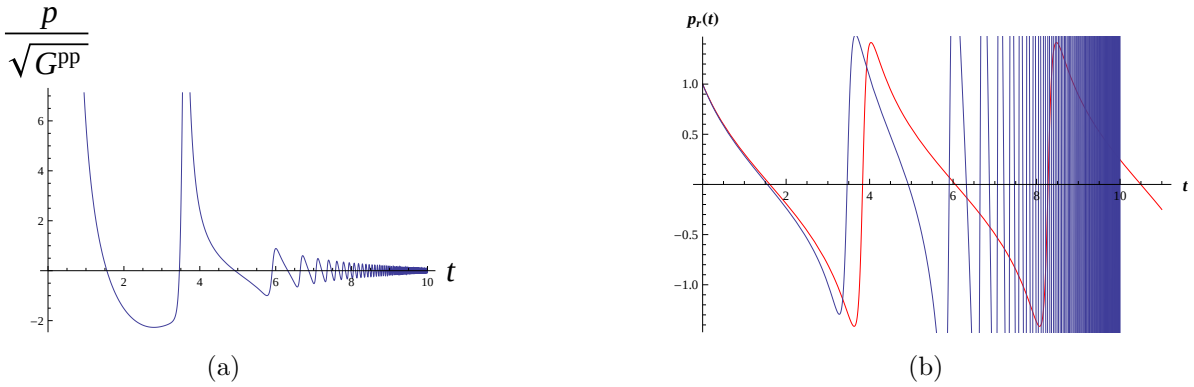

(a) (b)

Figure 5. (a) Plot of $p_r/\sqrt{G^{pp}}$ and (b) of the radial momentum, both with the same initial conditions as in Fig. 4.

One can always impose initial conditions complying with the uncertainty principle (2) for each pair of conjugate variables. We can see this in Fig. 6 for the radius, Fig. 7 for the ratio of the corresponding dispersions and Fig. 8 for their momenta, taking for the dispersions initial conditions progressively smaller. Although the behavior is qualitatively similar to that shown in Fig. 4 and Fig. 5, we can notice that, for the initial conditions that fulfill the uncertainty relations, we have better control of the approximation. This is because the effective evolution is very close to the classical one. Indeed, the smaller the initial condition for the perturbation, the longer the effective trajectory remains close to the classical one. One can see this kind of behavior, where the classical orbits decay after some time, when one considers the hydrogen atom interacting with external fields [17].

It is expected that the energy of the system is also back-reacted, which indeed is verified from the definition of the effective quantum energy (16). However, as classically

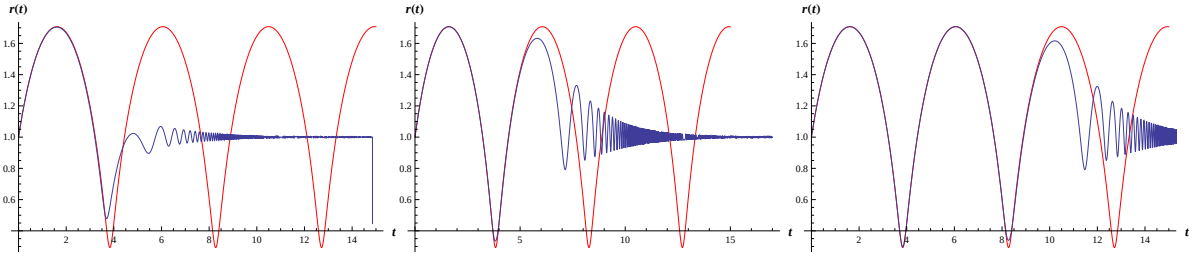

(a) (b) (c)

Figure 6. Plots of the radius as a function of time for initial conditions fulfilling the uncertainty relation (2). (a) Dispersions of order 0.001, (b) order 10^{-4} and (c) 10^{-5}. We can see that the smaller the perturbations, the longer they remain near the classical trajectory, allowing longer perturbation regions.

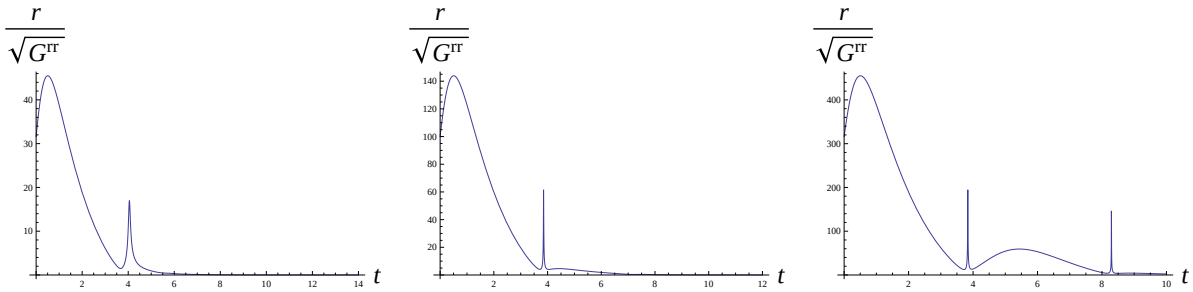

(a) (b) (c)

Figure 7. Plots of the ratio $r/\sqrt{G^{rr}}$ as a function of time for the same initial conditions as in Fig. 6. Interestingly, for these initial conditions the graph presents some peaks which indicates that dispersions may be considered as perturbations around those regions.

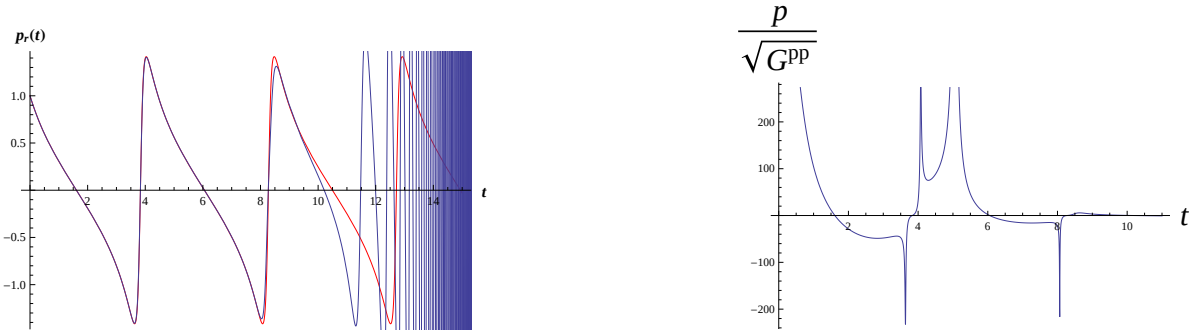

(a) (b)

Figure 8. (a) Plot of p_r and (b) $p_r/\sqrt{G^{pp}}$, for initial conditions of dispersions of order 10^{-5}. There are piecewise regions where the perturbative approximation is well suited.

the energy is a constant of motion, in the perturbative regime the effective behavior of the corrected energy oscillates about the classical energy with small amplitudes that depend on the initial conditions for the dispersions, as shown in Fig. 9.

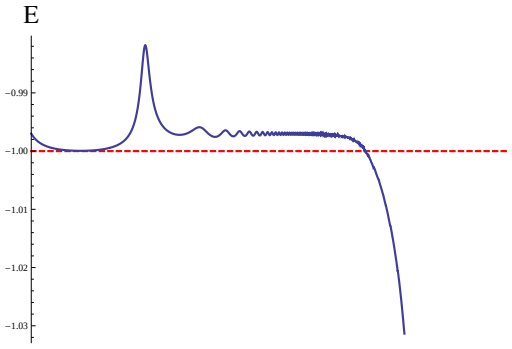

Figure 9. The classical (dashed red line) and quantum corrected (solid blue line) energy as function of time. The initial conditions for dispersions are of order 0.001.

Let us recall that classically the solution of the Kepler problem corresponds to a conic-section orbit whose eccentricity and perihelion depends on the energy and angular momentum. Although in the quantum-corrected study that we are discussing (as in any quantum/statistical description) one cannot have a closed analytical expression for the effective orbit, one can solve the system (22)-(34) numerically. With initial conditions fulfilling the uncertainty relations, we obtain an almost elliptical (open) orbit that is modified by the effect of back-reaction of quantum variables, as shown in Fig. 10. Under these conditions the effective orbit starts very close to the classical one and, as it evolves, quantum effects increasingly drive it away.

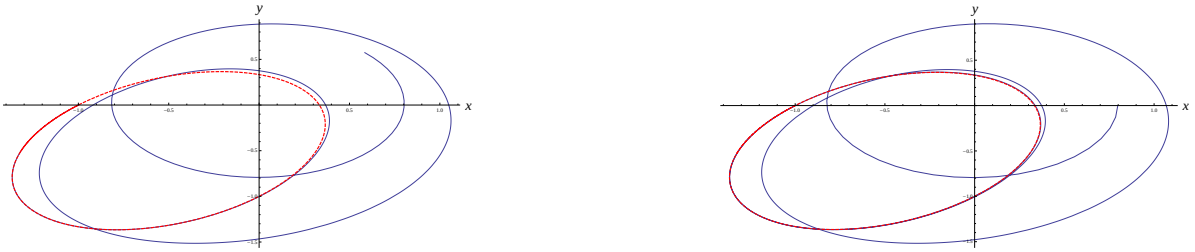

(a) (b)

Figure 10. The classical (dashed red line) and quantum corrected (solid blue line) orbits for dispersions of order (a) 10^{-4} and (c) 10^{-5}. Classical and quantum-corrected orbits starts close, but at large times the effective one spreads away.

The departure of the effective orbit from the classical one can also be understood by looking at the uncertainties in r. These are the curves located at each side of the quantum trajectory $r(\theta)$, (i.e. the brown and purple thin curves). in Fig. 11. Here we notice how, at the beginning of evolution, both the effective and classical orbits are within the range of dispersions $\pm\sqrt{G^{rr}} = \pm\Delta r$. As the system evolves we can see how the uncertainties start to grow and disperse. Interestingly at some point the uncertainties decrease and we recover the effective trajectory. For large initial conditions of the uncertainties this does not happen very close to the classical trajectory, but as one decreases the initial values this happens closer to the classical behavior,

Fig. 11. Actually, from the previous discussion we know that there is a region where the magnitude of the dispersion is comparable to that of the expectation values. Then we can interpret these as the quantum effects that keep the orbit away from the classical trajectory for large times. This behavior is similar to the one in [18], where minimum uncertainty states were constructed in which the wave function can be described by classical equations for short times, while for longer times the wave packet that lives in the elliptical trajectory begins to spread.

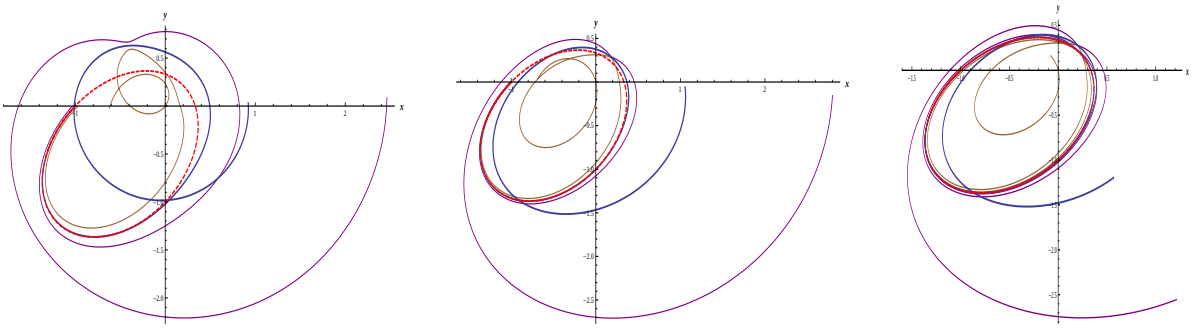

(a) (b) (c)

Figure 11. Plot of the quantum-corrected (blue) orbit surrounded by the corresponding dynamical uncertainties $r \pm \Delta r$ (thin curves), for initial conditions of the dispersions of order (a) 0.001, (b) 10^{-4} and (c) 10^{-5}. Also the classical orbit (red dashed curve) is shown. Initially the uncertainties are close to, and at each side of, the effective orbit, then they start to disperse. At large times they diverge completely from the classical behavior.

We can further appreciate the quantum evolution of the system by looking at the corresponding radial phase space diagram. Classically, for a particle rotating in an elliptic orbit in configuration space, the radial phase diagram is a closed curve representing a bound state in which the particle attains a maximum and a minimum value of its radius from the force center (dashed (red) curve in Fig. 12a). The solid curve in Fig. 12a corresponds to the quantum-corrected evolution; we notice that the effective quantum behavior starts close to the classical diagram and then disperses. This diagram shows how the quantum effects make the effective system depart from the classical one. As time evolves we see that the radius becomes increasingly smaller and the radial momentum grows. Moreover, after a long enough period of time, we can see in Fig. 12b that, as the radius gets localized, the radial momentum disperses: this is a direct manifestation of the uncertainty principle in phase space.

Fig. 13 shows how the dispersions evolve and to what extent the uncertainty principle is fulfilled. From Fig. 13 we see that the inequality is satisfied for short times, during the phase where the expansion can be treated perturbatively, as mentioned above. There is only one region where the product presents a peak but then remains flat for some more time. For large times the perturbative assumption is no longer valid, as the product of uncertainties grow larger and larger. This is a similar behavior as the one presented by a radial squeezed state studied in [14], where the uncertainty product

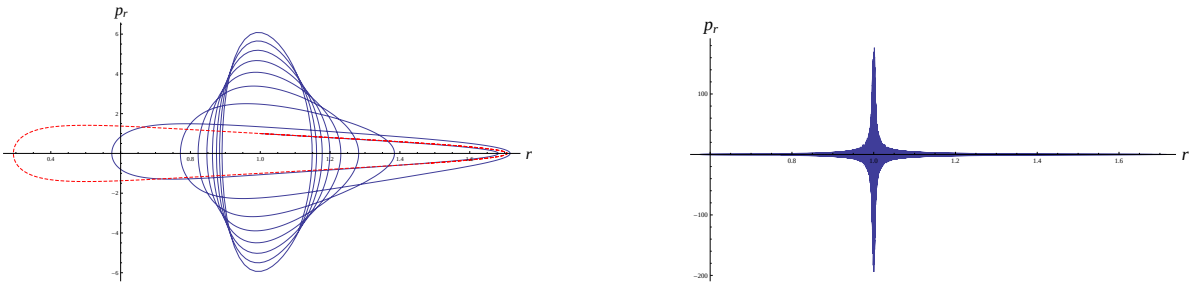

(a) (b)

Figure 12. (a) The dashed (red) line corresponds to the classical radial phase diagram while the solid (blue) curve is the effective quantum diagram for initial conditions of dispersions of order 0.01. (b) For later times the radial coordinate is fully localized while the radial momentum disperse completely.

features a cyclic behavior. In the same way we can say that our system begins in a state with minimum uncertainty, not squeezed, and for larger times it gets dispersed.

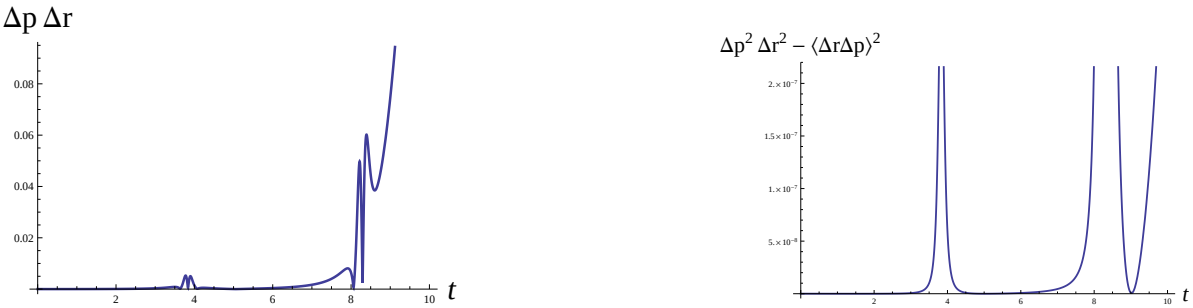

(a) (b)

Figure 13. The uncertainty relations (a) $\Delta r \Delta p_r$ and (b) $G^{rr}\ G^{p_r p_r} - (G^{r p_r})^2$ as function of time (order 10^{-5}). During the perturbative stage, the uncertainty relations are satisfied; for larger times the inequality is violated and quantum effects become increasingly dominant.

4.3. Different approaches to semi-classical limit of the Hydrogen atom

Even though the non-relativistic Hydrogen atom has been solved exactly it was latter proved that the WKB approximation was rather poor in this case, which is usually attributed to the singular behavior of the potential at the origin $r = 0$. It was shown in [15] that WKB can be performed in $r \to 0$ with precise results if the centrifugal term

$$V_C = \frac{\hbar^2 l(l+1)}{2mr^2}$$

is replaced by

$$V_C = \frac{\hbar^2 (l+1/2)^2}{2mr^2}$$

which in turn gives very accurate energy eigenvalues for the WKB approximation, even at lowest order. The main difference between WKB and the method presented here is the scope of the treatment: while both methods intend to establish a semiclassical approach to the quantum mechanical system at hand, the WKB aims at obtaining, by means of an series expansion on $\hbar$, the wave function and corrections to the energy levels. That is, one writes the wave function as [1]

$$\psi(\mathbf{r}) = e^{\frac{i}{\hbar}W(\mathbf{r})},$$

and the WKB approximation consists in expanding $W(\mathbf{r})$ in powers of $\hbar$ and in neglecting in the Schrödinger equation terms of order $\hbar^2$ or higher. Besides the fact that the method aims in approximating the wave function it fails in the vicinity of the *classical* turning points, i.e., $E = V(x)$. To circumvent this one defines the *connection* functions in order to connect the wave functions in the regions adjacent to the turning points.

Evolution and description of the quantum mechanical system in our method is not based on a wave function but rather in its momentous description and their quantum back-reaction on expectation values. One can compute the energy of the system and, probably the most interesting aspect of our description, also the semiclassical evolution of observables and orbits at different regimes in the parameter space. However, one feature that both schemes (and any approximation method in quantum mechanics) share is the growing in time of quantum corrections that render the approach invalid as well as the oscillatory character of the evolution in our case or in the expression of wave function and energy in the WKB. This is a well known effect in quantum mechanics.

The effective equations method presented here is an alternative method that in principle should reproduce all the results of standard quantum mechanics as long as one consider all the infinite moments. As mentioned, this method is quite suitable for a semi-classical analysis, defining a region where the moments can be considered as perturbations.

The semi-classical states of the Hydrogen atom have been explored in terms of the correspondence principle for large principal quantum number n. In such a case a wave packet can follow a classical orbit. Interestingly, given the conservation of energy and angular momentum, there are no transversal spreading in such states. The simplest of this states has a dispersion of order $n^{-1/2}$, and it evolves in such a way that the wave packet is distributed almost uniformly on a circular orbit [16]. The dynamics of these states have both classical and quantum features: for short times the motion is classical, after that the quantum dynamics becomes dominant [18]. Something very similar happens in our case, although we do not necessarily describe the same state, as the effective equations method provides us with minimal uncertainty dynamical states. There is also a formalism to construct radial and angular coherent and squeezed states that show the main features of classical motion [14, 19]. Semi-classical states have also been constructed from the coherent states of a 4 dimensional oscillator which is reached by the KS mapping of the 3 dimensional Hydrogen atom [20].

It is interesting to study the semi-classical states of the hydrogen atom as it has been possible to find them experimentally in the laboratory through the excitation of the outermost electrons of certain atoms, with ultrashort laser pulses [21]. Recently, there have been obtained experimentally new localized wave packets in very large n states that travel in nearly circular orbits [22].

The analysis presented here provides an alternative tool for the study of some different semi-classical states of the Hydrogen atom that had not been considered before, indeed we can see that our states are not of minimum uncertainty for all times. This is even clearer if we consider the ratio $\Delta r/\Delta p_r$ in Fig. 14. One can see that there is a group of peaks indicating that at those times the uncertainty in r increases as uncertainty in p_r decreases, while in the flat regions the opposite occurs. As in Fig. 13 we can compare this with the behavior of the radial squeezed state [14], where this ratio starts with a large amplitude and then damped oscillates until it reaches a minimum although continues oscillating, showing the squeezing in p_r. Clearly our state is not a squeezed one, but is the closest one that begins satisfying uncertainty relations.

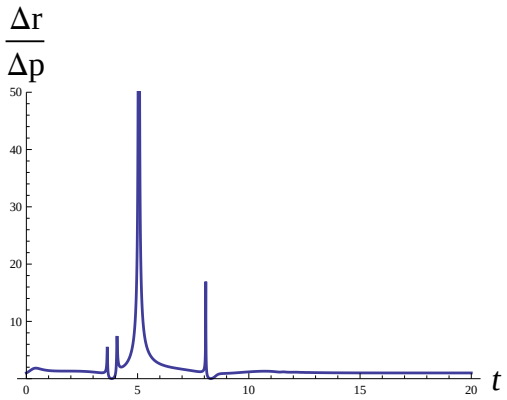

Figure 14. Ratio $\Delta r/\Delta p_r$. The peaks indicate that there is more spread in the radius than in the momentum at that time, i.e. states are squeezed for short periods.

5. Discussion

In this work we have obtained an effective description of the Hydrogen atom by means of a momentous formulation of quantum mechanics. We were able to obtain a semiclassical picture of the evolution of the classical dynamical variables by studying their equations of motion, back reacted by quantum dispersions and spreadings. This is done in regions where the moments can be considered as perturbations, which also allows us to make a consistent truncation of the equations of motion.

The equations of motion for expectation values are obtained from an effective Hamiltonian that acquires quantum corrections represented by spreadings to all orders. We have seen that the system reduces to the Kepler problem when one sets all the quantum fluctuations to zero. The case of zero angular orbital momentum, $l = 0$, that classically corresponds to a one dimensional system, gets so strongly quantum

corrected that it effectively corresponds to a two dimensional system. This behavior has no classical analogous, and in this way is a similar effect as the quantum tunneling phenomena.

The evolution of the system is controlled by generalizations of the Heisenberg uncertainty relations among quantum variables that are satisfied during the perturbative period, thus providing us with a consistent analysis and evolution.

As we pointed out we were able to determine the evolution of expectation values of variables which enabled us to determine an effective orbit for the electron, which is close to the classical elliptical orbit for short initial times. For larger times it is diverted to an open quasi-elliptical orbit as shown in Figs. 10, 11 and 12. One can see from these figures how quantum effects modify the classical behavior, realizing that, as the system evolves, there is a switching between the radial and momentum spreadings. It is interesting to point out that the behavior of the orbits and the spreadings shown in Fig. 11, although not identical, are similar to those reported in the literature where the wave packets follow elliptical orbits for a while and then spread.

Although this method gives a semi-classical behavior in a well-defined region, the states that we use are not the minimum uncertainty states that are usually called coherent states for the Hydrogen atom, or the Rydberg-type states similar to those that have been experimentally produced through ultra-short laser pulses. Our states are new states describing the semiclassical behavior of the Hydrogen atom. Thus we emphasize the qualitative features of this analysis, the method of effective equations and its robustness in obtaining new states suited to describe the semiclassical behavior.

Even though we were able to solve numerically the equations of motion, and with this obtaining the evolution of the system providing a rather interesting description, it is still needed to obtain a set of physical initial conditions that will allow us to compare quantitatively our results with experimental or theoretical data in a consistent manner. Due to the very complicated nature of the dynamical system and the infinite number of quantum variables this task is yet under further study.

Due to the complexity of the effective variables and their equations of motion we restricted ourselves to the two dimensional case, corresponding to the classical version, and then it is necessary to explore the three dimensional system. Given the results obtained in the one dimensional case, where quantum effects induce a two dimensional behavior, we could obtain modifications to the two dimensional motion due to quantum back-reaction by considering the remaining angular variable and its associated momenta, fixed in the present analysis. In such case the corresponding results should be more accurate and closer to those currently reported in the literature and experimentally.

The implications and possible applications of our analysis to other systems and phenomena are promising. For instance, the implementation of this method to Hydrogen-like atoms and systems should be straightforward and may result in a more detailed description and a deeper understanding of those systems. Note that, even for the Helium atom (a system with two electrons), there is no exact solution, and any study of this system is performed at an approximation level, being ours one that could

led to a more refined and precise description.

ACKNOWLEDGEMENTS

This work was supported by grant CONACYT CB-2008-01/101774.

Appendix A. Higher order moments

As shown in [8], as one considers higher order moments the average number of terms in the equations increases exponentially. Here we show the system of effective evolution equations up to third order, that corresponds to thirty coupled equations

$$\dot{p_r} = \frac{l^2}{mr^3} - \frac{k}{r^2} + \frac{\Delta l^2}{mr^3} + \frac{3}{r^4}G^{2,0,0,0}\left[\frac{l^2}{m}\frac{2}{r} - k\right] - \frac{4}{r^5}G^{3,0,0,0}\left[\frac{l^2}{m}\frac{5}{r} - k\right] - \frac{6}{mr^4}\left(lG^{1,0,0,1} + \frac{1}{2}G^{1,0,0,2}\right) + \frac{12\,l}{mr^5}G^{2,0,0,1}, \tag{A.1}$$

$$\dot{\theta} = \frac{l}{mr^2} - \frac{2}{mr^3}G^{1,0,0,1} + \frac{3}{mr^4}\left(lG^{2,0,0,0} + G^{2,0,0,1}\right) - \frac{4l}{mr^5}G^{3,0,0,0}, \tag{A.2}$$

$$\dot{G}^{1,1,0,0} = -\frac{1}{m}G^{0,2,0,0} + \left[\frac{3l^2}{2mr} - k\right]\frac{2}{r^3}G^{2,0,0,0} - \left[\frac{2l^2}{mr} - k\right]\frac{3}{r^4}G^{3,0,0,0} - \frac{2}{mr^3}\left(lG^{1,0,0,1} + \frac{1}{2}G^{1,0,0,2}\right) + \frac{6lG^{2,0,0,1}}{mr^4}, \tag{A.3}$$

$$\dot{G}^{0,2,0,0} = 4\left[\frac{3l^2}{2mr} - k\right]\frac{1}{r^3}G^{1,1,0,0} - 6\left[\frac{2l^2}{mr} - k\right]\frac{1}{r^4}G^{2,1,0,0} - \frac{2}{mr^3}\left(2lG^{0,1,0,1} + G^{0,1,0,2}\right) + \frac{12l}{mr^4}G^{1,1,0,1}, \tag{A.4}$$

$$\dot{G}^{0,0,1,1} = -\frac{\Delta l^2}{mr^2} + \frac{2}{mr^3}\left(lG^{1,0,0,1} + G^{1,0,0,2}\right) - \frac{3l}{mr^4}G^{2,0,0,1}, \tag{A.5}$$

$$\dot{G}^{0,0,2,0} = -\frac{2}{mr^2}G^{0,0,1,1} + \frac{4}{mr^3}\left(lG^{1,0,1,0} + G^{1,0,1,1}\right) - \frac{6l}{mr^4}G^{2,0,1,0}, \tag{A.6}$$

$$\dot{G}^{1,0,1,0} = -\frac{1}{m}G^{0,1,1,0} - \frac{1}{mr^2}G^{1,0,0,1} + \frac{2}{mr^3}\left(lG^{2,0,0,0} + G^{2,0,0,1}\right) - \frac{3l}{mr^4}G^{3,0,0,0}, \tag{A.7}$$

$$\dot{G}^{0,1,0,1} = \left[\frac{3l^2}{2mr} - k\right]\frac{2}{r^3}G^{1,0,0,1} - \left[\frac{2l^2}{mr} - k\right]\frac{2}{r^4}G^{2,0,0,1} - \frac{1}{mr^3}\left(2l\Delta l^2 - G^{0,0,0,3}\right) + \frac{6l}{mr^4}G^{1,0,0,2}, \tag{A.8}$$

$$\dot{G}^{0,1,1,0} = -\frac{1}{mr^2}G^{0,1,0,1} + \left[\frac{3l^2}{2mr} - k\right]\frac{2}{r^3}G^{1,0,1,0} + \frac{1}{mr^3}\left[2l\left(G^{1,1,0,0} - G^{0,0,1,1}\right)\right] - \left(G^{0,0,1,2} - 2G^{1,1,0,1}\right) - \left[\frac{2l^2}{mr} - k\right]\frac{3}{r^3}G^{2,0,1,0} + \frac{3l}{mr^4}\left(2G^{1,0,1,1} - G^{2,1,0,0}\right) \tag{A.9}$$

We omit equations for r, p_θ, $G^{2,0,0,0}$ and $G^{1,0,0,1}$ because they are not modified with respect to previous expressions of second order. Also we replace $G^{0,0,0,2}$ with Δl^2.

Beside this system there are another eighteen equations:

$$\dot{G}^{1,1,1,0} = -\frac{G^{0,2,1,0}}{m} - \frac{G^{1,1,0,1}}{mr^2} + \frac{3}{r^4}\left[-k + \frac{2l^2}{mr}\right] G^{1,0,1,0}G^{2,0,0,0} + \frac{2}{r^3}\left[-k + \frac{3l^2}{2mr}\right] G^{2,0,1,0}$$
$$+\frac{3}{mr^4}\left[l(-2G^{1,0,0,1}G^{1,0,1,0} + G^{1,1,0,0}G^{2,0,0,0}) - (G^{1,0,0,2}G^{1,0,1,0} - G^{1,1,0,0}G^{2,0,0,1})\right]$$
$$-\frac{1}{mr^3}2\left[\frac{1}{2}(-\Delta l^2 G^{1,0,1,0} + 2G^{1,0,0,1}G^{1,1,0,0}) + l(G^{1,0,1,1} - G^{2,1,0,0})\right], \tag{A.10}$$

$$\dot{G}^{1,1,0,1} = -\frac{G^{0,2,0,1}}{m} + \frac{(\Delta l^2 G^{1,0,0,1} - 2lG^{1,0,0,2})}{mr^3} - \frac{3\left(2l(G^{1,0,0,1})^2 + G^{1,0,0,1}G^{1,0,0,2}\right)}{mr^4}$$
$$+\frac{3}{r^4}\left(-k + \frac{2l^2}{mr}\right) G^{1,0,0,1}G^{2,0,0,0} + \frac{2}{r^3}\left(-k + \frac{3l^2}{2mr}\right) G^{2,0,0,1}, \tag{A.11}$$

$$\dot{G}^{1,0,1,1} = -\frac{G^{0,1,1,1}}{m} - \frac{G^{1,0,0,2}}{mr^2} + \frac{3(lG^{1,0,0,1}G^{2,0,0,0} + G^{1,0,0,1}G^{2,0,0,1})}{mr^4}$$
$$-\frac{2\left((G^{1,0,0,1})^2 - lG^{2,0,0,1}\right)}{mr^3}, \tag{A.12}$$

$$\dot{G}^{0,1,1,1} = -\frac{G^{0,1,0,2}}{mr^2} + \frac{2}{r^3}\left[-k + \frac{3l^2}{2mr}\right] G^{1,0,1,1} + \frac{3}{r^4}\left[-k + \frac{2l^2}{mr}\right] G^{0,0,1,1}G^{2,0,0,0}$$
$$+\frac{3}{mr^4}\left[l(-2G^{0,0,1,1}G^{1,0,0,1} + G^{0,1,0,1}G^{2,0,0,0}) - (G^{0,0,1,1}G^{1,0,0,2} - G^{0,1,0,1}G^{2,0,0,1})\right]$$
$$-\frac{1}{mr^3}\left[(-\Delta l^2 G^{0,0,1,1} + 2G^{0,1,0,1}G^{1,0,0,1}) + 2l(G^{0,0,1,2} - G^{1,1,0,1})\right], \tag{A.13}$$

$$\dot{G}^{1,2,0,0} = -\frac{G^{0,3,0,0}}{m} - \frac{3(4lG^{1,0,0,1}G^{1,1,0,0} + 2G^{1,0,0,2}G^{1,1,0,0})}{mr^4} + \frac{2(\Delta l^2 G^{1,1,0,0} - 2lG^{1,1,0,1})}{mr^3}$$
$$+\frac{6}{r^4}\left[-k + \frac{2l^2}{mr}\right] G^{1,1,0,0}G^{2,0,0,0} + \frac{4}{r^3}\left[-k + \frac{3l^2}{2mr}\right] G^{2,1,0,0}, \tag{A.14}$$

$$\dot{G}^{1,0,2,0} = -\frac{G^{0,1,2,0}}{m} + \frac{6G^{1,0,1,0}(lG^{2,0,0,0} + G^{2,0,0,1})}{mr^4} - \frac{4(G^{1,0,0,1}G^{1,0,1,0} - lG^{2,0,1,0})}{mr^3}, \tag{A.15}$$

$$\dot{G}^{1,0,0,2} = -\frac{G^{0,1,0,2}}{m}, \tag{A.16}$$

$$\dot{G}^{0,1,0,2} = \frac{((\Delta l^2)^2 - 2lG^{0,0,0,3})}{mr^3} + \frac{2}{r^3}\left[-k + \frac{3l^2}{2mr}\right] G^{1,0,0,2} + \frac{3}{r^4}\left[-k + \frac{2l^2}{mr}\right] \Delta l^2 G^{2,0,0,0}$$
$$-\frac{3\Delta l^2(2lG^{1,0,0,1} + G^{1,0,0,2})}{mr^4},$$

$$\dot{G}^{0,1,2,0} = -\frac{2G^{0,1,1,1}}{mr^2} + \frac{2}{r^3}\left[-k + \frac{3l^2}{2mr}\right] G^{1,0,2,0} + \frac{3}{r^4}\left[-k + \frac{2l^2}{mr}\right] G^{0,0,2,0}G^{2,0,0,0}$$
$$-\frac{2}{mr^3}\left[\left(2G^{0,1,1,0}G^{1,0,0,1} - \Delta l^2 G^{0,0,2,0} + \frac{i\hbar}{2}\{G^{1,1,0,0} - 2G^{0,0,1,1}\}\right)\right.$$
$$\left.+l(G^{0,0,2,1} - 2G^{1,1,1,0})\right] + \frac{3}{mr^4}\left[\left(2G^{0,1,1,0}G^{2,0,0,1} - G^{0,0,2,0}G^{1,0,0,2}\right.\right.$$
$$\left.\left.+\frac{i\hbar}{2}\{G^{2,1,0,0} - 4G^{1,0,1,1}\}\right) + 2l(G^{0,1,1,0}G^{2,0,0,0} - G^{0,0,2,0}G^{1,0,0,1})\right], \tag{A.17}$$

$$\dot{G}^{0,2,0,1} = \frac{2(\Delta l^2 G^{0,1,0,1} - 2lG^{0,1,0,2})}{mr^3} - \frac{6(2lG^{0,1,0,1}G^{1,0,0,1} + G^{0,1,0,1}G^{1,0,0,2})}{mr^4}$$

$$+\frac{4}{r^3}\left[-k+\frac{3l^2}{2mr}\right]G^{1,1,0,1}+\frac{6}{r^4}\left[-k+\frac{2l^2}{mr}\right]G^{0,1,0,1}G^{2,0,0,0}, \tag{A.18}$$

$$\begin{aligned}\dot{G}^{0,2,1,0} = &-\frac{G^{0,2,0,1}}{mr^2}-\frac{4}{r^3}\left[k-\frac{3l^2}{2mr}\right](G^{1,1,1,0}-G^{0,1,1,0}G^{1,0,0,0})-\frac{6}{r^4}\left[k-\frac{2l^2}{mr}\right]G^{0,1,1,0}G^{2,0,0,0}\\ &-\frac{2}{mr^3}\left[(G^{0,2,0,0}G^{1,0,0,1}-\Delta l^2 G^{0,1,1,0})+l(2G^{0,1,1,1}-G^{1,2,0,0})\right]\\ &+\frac{3}{mr^4}\Bigg[l(G^{0,2,0,0}G^{2,0,0,0}-4G^{0,1,1,0}G^{1,0,0,1}+i\hbar\{G^{0,0,1,1}-2G^{1,1,0,0}\})\\ &+\left(G^{0,2,0,0}G^{2,0,0,1}-2G^{0,1,1,0}G^{1,0,0,2}+\frac{i\hbar}{2}\{G^{0,0,1,2}-4G^{1,1,0,1}\}\right)\Bigg],\end{aligned} \tag{A.19}$$

$$\dot{G}^{2,0,0,1} = -\frac{2G^{1,1,0,1}}{m}, \tag{A.20}$$

$$\dot{G}^{2,0,1,0} = -\frac{2G^{1,1,1,0}}{m}-\frac{G^{2,0,0,1}}{mr^2}+\frac{3\left(l(G^{2,0,0,0})^2+G^{2,0,0,0}G^{2,0,0,1}\right)}{mr^4}-\frac{2(G^{1,0,0,1}G^{2,0,0,0}-lG^{3,0,0,0})}{mr^3}, \tag{A.21}$$

$$\begin{aligned}\dot{G}^{2,1,0,0} = &-\frac{2G^{1,2,0,0}}{m}+\frac{3}{r^4}\left[-k+\frac{2l^2}{mr}\right](G^{2,0,0,0})^2+\frac{2}{r^3}\left[-k+\frac{3l^2}{2mr}\right]G^{3,0,0,0}\\ &+\frac{(\Delta l^2 G^{2,0,0,0}-2lG^{2,0,0,1})}{mr^3}-\frac{3(2lG^{1,0,0,1}G^{2,0,0,0}+G^{1,0,0,2}G^{2,0,0,0})}{mr^4},\end{aligned} \tag{A.22}$$

$$\dot{G}^{0,0,0,3} = 0, \tag{A.23}$$

$$\dot{G}^{0,0,3,0} = -\frac{3G^{0,0,2,1}}{mr^2}-\frac{6(G^{0,0,2,0}G^{1,0,0,1}-lG^{1,0,2,0})}{mr^3}+\frac{9(lG^{0,0,2,0}G^{2,0,0,0}+G^{0,0,2,0}G^{2,0,0,1})}{mr^4}, \tag{A.24}$$

$$\begin{aligned}\dot{G}^{0,3,0,0} = &\frac{(3\Delta l^2 G^{0,2,0,0}-6lG^{0,2,0,1})}{mr^3}+\frac{6}{r^3}\left[-k+\frac{3l^2}{2mr}\right]G^{1,2,0,0}\\ &-\frac{9(2lG^{0,2,0,0}G^{1,0,0,1}+G^{0,2,0,0}G^{1,0,0,2})}{mr^4}+\frac{9}{r^4}\left[k-\frac{2l^2}{mr}\right](i\hbar G^{1,1,0,0}-G^{0,2,0,0}G^{2,0,0,0}),\end{aligned} \tag{A.25}$$

$$\dot{G}^{3,0,0,0} = -\frac{3G^{2,1,0,0}}{m}. \tag{A.26}$$

From (A.23) we immediately see that $G^{0,0,0,3}$ is a constant, as we already noticed for the moments of $G^{0,0,0,n}$ to any order n.

References

[1] E. Merzbacher, *Quantum Mechanics*, 2nd edition Wiley, New York, (1970).

[2] M. Bojowald and A. Skirzewski, Rev. Math. Phys. **18**, 713 (2006).

[3] F. Cametti, G. Jona-Lasinio, C. Presilla and F. Toninelli In Proceedings of the International School of Physics "Enrico Fermi", Course CXLIII, Ed. G. Casati, I. Guarneri, U. Smilansky (IOS Press, Amsterdam 2000), p. 431-448 (quant-ph/9910065); W. Heisenberg, H. Euler, Zeitschr. Phys. **98**, 714 (1936), (physics/0605038).

[4] N. C. Dias, A. Mikovic, and J. N. Prata, J. Math. Phys. (N.Y.) **47**, 082101 (2006).

[5] M. Bojowald, Phys. Rev. D **75**, 081301(R) (2007); M. Bojowald, Phys. Rev. D **75**, 123512 (2007).

[6] M. Bojowald, Nature Physics **3**, 523 (2007).

[7] M. Bojowald, H. H. Hernández and A. Skirzewski, Phys. Rev. D **76**, 063511 (2007).

[8] M. Bojowald, D. Brizuela, H. H. Hernández, M. J. Koop and H. A. Morales-Técotl, Phys. Rev. D **84**, 043514 (2011).

[9] M. Bojowald, M. Kagan, H. H. Hernández, A. Skirzewski, Phys. Rev. D **75**, 064022 (2007); M. Bojowald and A. Tsobanjan, Phys. Rev. D **80**, 125008 (2009).
[10] M. Bojowald, arXiv:1101.5592, (2011).
[11] P.A.M. Dirac, *The Principles of Quantum Mechanics*, First edition, Oxford Clarendon Press, (1930).
[12] R. Loudon, Am. J. Phys. **27**, 649 (1959); H. N. Núñez-Yépez, A. L. Salas-Brito, D. A. Solis, Phys. Rev. A **83**, 064101 (2011).
[13] M. Mayle, B. Hezel, I. Lesanovsky and P. Schmelcher, Phys. Rev. Lett. **99**, 113004 (2007); M. M. Nieto, Phys. Rev. A **61**, 034901 (2000); C. D. Schwieters and J. B. Delos, Phys. Rev. A **51**, 1030 (1995).
[14] R. Bluhm and V. A. Kostelecký, Phys. Rev. A **48**, R4047 (1993); R. Bluhm, V. A. Kostelecký and B. Tudose, Phys. Rev. A **52**, 2234 (1995).
[15] R. Langer, Phys. Rev. **59** 669, (1937).
[16] L. S. Brown, Am. J. Phys. **41**, 525 (1973);
[17] D. C. Cole and Yi Zou, Phys. Rev. E **69**, 016601 (2004).
[18] Z. D. Gaeta and C. S. Stroud Jr., Phys. Rev. A **42**, 6308 (1990).
[19] M. M. Nieto, Phys. Rev. D **22**, 391 (1980).
[20] D. Bhaumik, B. D. Dutta-Roy and G. Ghosh, J. Phys. A: Math. Gen. **19**, 1355 (1986); S. Nandi and C. S. Shastry, J. Phys. A: Math. Gen. **22**, 1005 (1989); A. Rauh and J. Parisi, Phys. Rev. A **83**, 042101 (2011).
[21] J. Parker and C. S. Stroud Jr., Phys. Rev. Lett. **56**, 716 (1986); J. Parker and C. S. Stroud, Phys. Scripta T12, 70 (1986); J. A. Yeazell and C. S. Stroud Jr., Phys. Rev. Lett. **60**, 1494 (1988); J. A. Yeazell and C. S. Stroud Jr., Phys. Rev. A **43**, 5153 (1991).
[22] J. J. Mestayer, B. Wyker, J. C. Lancaster, F. B. Dunning, C. O. Reinhold, S. Yoshida, and J. Burgdörfer, Phys. Rev. Lett. **100**, 243004 (2008); H. Maeda, J. H. Gurian, and T. F. Gallagher, Phys. Rev. Lett. **102**, 103001 (2009); J. J. Mestayer, B. Wyker, F. B. Dunning, S. Yoshida, C. O. Reinhold, and J. Burgdörfer Phys. Rev. Lett. **79**, 033417 (2010).